



Characteristics of Ground Vibrations Induced by Teleseismic Earthquakes and Their Impact on Vibration-Sensitive Facilities

Yung-Yen Ko & Chun-Hsiang Kuo

To cite this article: Yung-Yen Ko & Chun-Hsiang Kuo (2022): Characteristics of Ground Vibrations Induced by Teleseismic Earthquakes and Their Impact on Vibration-Sensitive Facilities, Journal of Earthquake Engineering, DOI: [10.1080/13632469.2021.1991526](https://doi.org/10.1080/13632469.2021.1991526)

To link to this article: <https://doi.org/10.1080/13632469.2021.1991526>



Published online: 13 Jan 2022.



Submit your article to this journal [↗](#)



Article views: 41



View related articles [↗](#)



View Crossmark data [↗](#)



Characteristics of Ground Vibrations Induced by Teleseismic Earthquakes and Their Impact on Vibration-Sensitive Facilities

Yung-Yen Ko^a and Chun-Hsiang Kuo^{b,c,d}

^aDepartment of Civil Engineering, National Cheng Kung University, Tainan, Taiwan; ^bDepartment of Earth Sciences, National Central University, Taoyuan, Taiwan; ^cEarthquake-Disaster & Risk Evaluation and Management Center, National Central University, Taoyuan, Taiwan; ^dNational Center for Research on Earthquake Engineering, National Applied Research Laboratories, Taipei, Taiwan

ABSTRACT

The ground vibrations observed in Taiwan during three teleseismic earthquakes in 2011 by broadband seismometers near major science parks were investigated. Their frequency content was exhibited via spectral analysis, and their effect on structures was examined by response spectra. To assess their possible impact on vibration-sensitive facilities, three vibration criteria in terms of velocity or displacement were utilized. Their predominant frequencies were between 0.04– and 0.16 Hz and somewhat dependent on focal depth and site geology, and they were therefore only influential to very long-period structures. However, the vibration levels exceeded the adopted criteria to some extent, especially at the softer site.

ARTICLE HISTORY

Received 3 April 2021
Accepted 24 September 2021

KEYWORDS



Ground vibration; teleseismic earthquake; frequency content; response spectrum; vibration criteria

1. Introduction

Teleseismic earthquakes denote those with sources very far away, at distances greater than 1,000 km from the measurement site according to the definition of United States Geological Survey (USGS 2021). Teleseismic waves can be used to identify the internal structure of the Earth, that is, teleseismic tomography, e.g. Rawlinson et al. (2016) and Estève et al. (2020), because they propagate deep inside the Earth. In addition, teleseismic wave propagation in deeper parts of the Earth is more regular than in the crust and can thus be described sufficiently well by 1-D velocity and attenuation models, which permits derivation of globally applicable teleseismic magnitude scales (Bormann et al. 2013) such as surface-wave magnitude (M_s) (Gutenberg 1945a) and body-wave magnitude (m_b) (Gutenberg 1945b, 1945c).

The ground vibration caused by a teleseismic earthquake, also known as the teleseism, is usually low-frequency-dominant because the high-frequency content decays more easily during the propagation and possible multiple reflections in the crust. Besides, its shaking is usually imperceptible to human body and can only be detected by broadband seismometers at quiet sites. However, for deep (hundreds of kilometers) and large-magnitude teleseismic earthquakes, felt reports came from thousands of kilometers away, possibly due to the lengthy, long-period (>3 sec) ground motions from the S phase of seismic waves and its multiple reflections as well as relevant phases that carried energy to considerable distances along with amplification by sedimentary basins and tall buildings (Furumura and Kennett 2019).

Teleseisms are known to induce abrupt fluctuations of groundwater levels and pressures, e.g. Liu, Huang, and Tsai (2006) and Barberio et al. (2020). On the other hand, they are generally insufficient to cause structural and non-structural damage or disorder due to their very low intensity; e.g. for example, Furumura and Kennett (2019) indicated that a felt reports of the 2013

CONTACT Yung-Yen Ko  yyko@ncku.edu.tw  Department of Civil Engineering, National Cheng Kung University, No.1 University Road, Tainan 70101, Taiwan

This article has been republished with minor changes. These changes do not impact the academic content of the article.

Sea of Okhotsk earthquake with a moment magnitude (M_w) of 8.3 at an epicentral distance of 6,105 km were as related to an intensity smaller than the threshold of the lowest level of the intensity scale for long-period ground motions proposed by Japan Meteorological Agency (JMA) for assessing their effect on high-rise buildings (Sakai 2015), which is in terms of absolute velocity response spectrum. Nevertheless, teleseisms could be influential regarding the serviceability of facilities because equipment in those for high technology and advanced research, such as fabs for semiconductor manufacturing and particle accelerators for high-energy physics (e.g. colliders and synchrotron light sources), might be very sensitive to vibrations for its micro-to-nano-scale precision requirement.

During the extremely disastrous 2011 off the Pacific coast of Tohoku earthquake (M_w 9.1), also known as the Great East Japan earthquake, the felt report indicated that weak to light shaking was perceived in both northern and southern Taiwan (over 2,000 km from the epicenter) (USGS 2021). This implied the potential of this teleseismic event to affect vibration-sensitive facilities in Taiwan, such as those in the semiconductor industry, which has become the pillar of Taiwan's economy in recent years. Since the influence of teleseismic earthquakes has rarely been studied from the engineering point of view, the aforementioned phenomenon motivated us to characterize the teleseisms and reveal its possible impact of on vibration-sensitive facilities.

In this study, we investigated the records at two stations of the Broadband Seismographic System of Central Weather Bureau (CWB), Taiwan, during three representative teleseismic events in 2011, including the Great East Japan earthquake, its largest aftershock, and another major one in Myanmar with a different focal mechanism. These records were provided by the Geophysical Database Management System (GDMS) of CWB (CWB 2021; Shin et al. 2013). The two stations are near Hsinchu Science Park and Tainan Science Park, respectively, both of great importance to the high-tech industries in Taiwan. The spectrum analysis based on Fourier transform was firstly performed to show the frequency content of these teleseisms. Then, the response spectra in terms of spectral acceleration, velocity and displacement were generated to evaluate their influence on structures. Finally, the one-third octave band root-mean-square (RMS) velocity and the integrated RMS displacement of the observed teleseisms were compared with three widely used vibration criteria for vibration-sensitive facilities so that their possible ill effects can be exhibited. Results of this study can not only highlight the need to include the effects of teleseisms in the design and operation of vibration-sensitive facilities, but also serve as the preliminary reference for setting the target of vibration mitigation as well as establishing the emergency operating procedure for these facilities.

2. Data Collection, Processing and Interpretation

2.1. Teleseismic Earthquake Events

Three teleseismic earthquakes were selected in this study, of which the locations of epicenters are given in Fig. 1. Their information is briefed in Table 1 and described as follows.

The first event is the 2011 off the Pacific coast of Tohoku earthquake on March 11, 2011, which had a magnitude of M_w 9.1 (originally reported M_w 9.0 and was updated in 2016) and an epicenter located at 38.297°N 142.373°E with a focal depth of 29.0 km (USGS 2021). This event was a large-scale subduction zone earthquake corresponding to a finite-fault plane with large slip approximately 150-km wide by 300-km long (Ammon et al. 2011), and the strong ground motions were actually originated from three large slips and therefore multiple shocks were clearly observed at some of the stations (Furumura et al. 2011). Devastating tsunami that travelled across the Pacific basin was therefore caused, leading to nearly 20,000 deaths and enormous destruction to affected costal area in Japan as well as some damage in other countries (Dengler and Sugimoto 2011). In addition, considerable ground shaking lasting several minutes was observed over a wide area of Japan, which had a large peak ground acceleration (PGA) up to

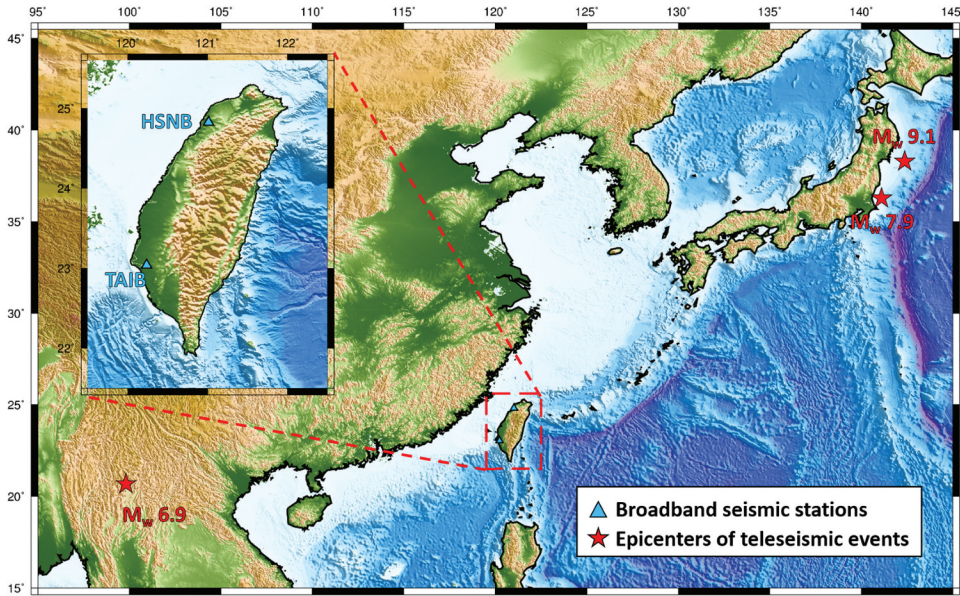


Figure 1. Locations of epicenters of investigated teleseismic events and adopted broadband seismic stations in Taiwan.

Table 1. Information of investigated teleseismic earthquakes (USGS 2021; CWB 2021).

Event	Date	M_w	Epicenter	Focal depth	Epicentral distance to broadband stations
2011 Great East Japan earthquake	March 11, 2011	9.1	38.297°N 142.373°E	29.0 km	HSNB 2,507 km TAIB 2,700 km
Largest aftershock of 2011 Great East Japan earthquake	March 11, 2011	7.9	36.281°N 141.111°E	42.6 km	HSNB 2,300 km TAIB 2,488 km
2011 Tarlay, Myanmar earthquake	March 24, 2011	6.9	20.687°N 99.822°E	8.0 km	HSNB 2,219 km TAIB 2,121 km

1–2 g and dominant periods <1 sec in northern Japan, whereas moderate PGA around 0.05–0.2 g and much longer periods of 6–8 sec in the Kanto (Tokyo) sedimentary basin (Furumura et al. 2011) were observed. The latter was related to the severe liquefaction of reclaimed lands in the Tokyo Bay area, though it was about 380–400 km from the epicenter and 110 km from the boundary of the rupture plane, because of the very long duration (Yasuda et al. 2012).

The second event is the largest aftershock of the first around half hour later on the very same day, which had a magnitude of M_w 7.9, an epicenter located at 36.281°N 141.111°E, and a focal depth of 42.6 km (USGS 2021). It exhibited a reverse fault type as the mainshock did (Hirose et al. 2011). Despite the considerable magnitude, the observed PGA was merely close to 0.2 g at the nearest inland station with an epicentral distance of 65 km (USGS 2021).

The third was a M_w 6.9 shallow earthquake (focal depth = 8.0 km) occurred in Tarlay, Myanmar, on March 24, 2011 with an epicenter at 20.687°N 99.822°E, and PGA near the epicenter was estimated beyond 0.2 g (USGS 2021). This event was caused by strike-slip faulting according to its focal mechanism (USGS 2021), and field measurements augmented by interpretation of satellite imagery indicated a surface rupture 30 km (Tun et al. 2014).

These three events are abbreviated as 2011 M_w 9.1 JPEQ, 2011 M_w 7.9 JPEQ, and 2011 M_w 6.9 MMEQ hereafter, respectively.

2.2. Broadband Seismic Stations

Two surface stations of the Broadband Seismographic System of CWB were adopted in this study, and their locations are shown in Fig. 1. One is HSNB station in Hsinchu, northern part of Taiwan (24.828° N 121.014°E), and it is only kilometers away from Hsinchu Science Park, where many high-tech factories and National Synchrotron Radiation Research Center which that has two synchrotron light sources are located. The ground of this site is composed of gravels with little silty sand above the depth of 12 m underlaid by thick sandstone and has a V_{S30} (averaged shear-wave velocity in the top 30 m of the ground, which is widely used as an indicator of site classification for seismic design) of 427.1 m/s (Kuo et al. 2012), which is categorized as class C site (very dense soil and soft rock) based on the NEHRP definitions (BSSC 2003). The other is TAIB station in Tainan, southern part of Taiwan (23.038°N 120.236°E), and it is less than 10 km from Tainan Science Park, which is more recently developed, larger than Hsinchu Science Park and is critical to high-tech industries in Taiwan. This station is rested on thick alluvium mainly composed of silty sand with $V_{S30} = 162.3$ m/s (Kuo et al. 2012), which is categorized as NEHRP class E site (soft soil) (BSSC 2003). The distances from both stations to the epicenters of the three investigated teleseismic earthquakes were all more than 2,000 km, as depicted in Table 1.

The broadband seismometer GÜRALP CMG-40TD was used at both HSNB and TAIB during the investigated teleseismic earthquakes with the sampling rate of 100 Hz. It has 24-bit digital outputs, a standard sensitivity of 2×400 V/ms⁻¹, a peak output of ± 10 V, a standard output bandwidth (flat response within -3 dB crossing points) of 0.033–50 Hz, and a lowest spurious resonance of 450 Hz (GÜRALP Systems 2021).

2.3. Data Processing Scheme

Firstly, instrument response correction with the pole-zero parameters of each CMG-40TD seismometer was made on all the teleseismic records utilized in this study. Thus, even though the seismometer had flat response to 0.033 Hz, the useable frequency range of the data can be lowered to 0.01 Hz for better characterizing the low-frequency content of the teleseisms.

Then, the teleseism data were band-pass filtered with a pass band of 0.01–50 Hz, which was determined based on the sampling rate, the velocity response of the seismometers, and also the fact that the ground vibrations with frequencies < 0.01 Hz are associated with very long wavelengths compared to the dimensions of facilities and thus have hardly any influence on them.

Beside the Fourier spectrum to exhibit the frequency content of the signals, two more spectral quantities were calculated to be compared with the vibration criteria introduced in the following section. One is the one-third octave band RMS velocity spectrum $\sigma_{1/3oct}(f_c^i)$, which can be obtained by velocity power spectrum density function $S_V(f)$:

$$\sigma_{1/3oct}(f_c^i) = \sqrt{\int_{f_l^i}^{f_u^i} S_V(f) df} = \sqrt{\frac{2}{T_p} \int_{f_l^i}^{f_u^i} |V(f)|^2 df} \quad (1)$$

where $V(f)$ is the Fourier spectrum of measured velocity, T_p is the period for Fourier transform, and f_c^i , f_u^i , and f_l^i are the center, upper-bound, and lower-bound frequencies of i -th one-third octave band. Additionally, in practice, $\sigma_{1/3oct}(f_c^i)$ is usually expressed in terms of velocity level (L_V) in decibels (dB), as defined in the following equation defines:

$$L_V = 20 \cdot \log \frac{\sigma_{1/3oct}(f_c^i)}{\sigma_0} \quad (2)$$

where σ_0 is the reference velocity amplitude and $\sigma_0 = 2.54 \times 10^{-6}$ cm/s is usually adopted (Hanson, Towers, and Meister 2006).

The other term often adopted for facilities sensitive to vibrational displacement such as that the particle accelerator is the integrated RMS displacement at a specified frequency f_k , $D_{RMS}(f_k)$, which helps to identify at what frequency range the vibration contributes more to displacement, is defined as:

$$D_{RMS}(f_k) = \sqrt{\int_{f=f_k}^{f=f_{max}} S_D(f) df} \quad (3)$$

where f_{max} corresponds to the largest measurable frequency, and $S_D(f)$ is the displacement power spectrum density function, which is defined as:

$$S_D(f) = \frac{1}{(2\pi f)^2} S_V(f) \quad (4)$$

In addition to the characteristics of the ground vibration itself, the excited structural response is as well also important to investigate its influence. Hence, the response spectrum (the plot of the maximum response to a given dynamic excitation for single degree-of-freedom systems with various natural frequencies) of each teleseism in terms of absolute spectral acceleration (S_a), absolute spectral velocity (S_{va}), and relative spectral displacement (S_d) will also be discussed. It is noted that S_{va} is used instead of a more common term, relative spectral velocity (S_v), because the results will be compared to the JMA intensity scale for long-period ground motions (Sakai 2015) mentioned in the introduction section.

2.4. Vibration Criteria

Firstly, to check if the teleseisms can cause any structural and non-structural damage or disorder, the JMA intensity scale for long-period ground motions in terms of S_{va} within the period range of 1.5–8 sec (Sakai 2015) is introduced. Its lowest level (level 1) is defined by $5 \text{ cm/s} \leq S_{va} < 15 \text{ cm/s}$, which can be felt by indoor people and can cause shaking of suspended objects such as window blinds. Level 2 is defined by $15 \text{ cm/s} \leq S_{va} < 50 \text{ cm/s}$, which can disturb people walking and move wheeled furniture. Cracks of partition wall can only be caused by a shaking above level 3, which is over 50 cm/s.

Then, the following criteria are utilized for the assessment of the impact of teleseismic earthquake-induced ground vibrations on vibration-sensitive facilities.

When designing facilities for research, manufacturing and other similar activities that need high precision, the generic vibration criterion (VC) curves are commonly used, which were developed in early 1980's for microelectronics manufacturing, originally known as the "BBN" (Bolt Beranek & Newman Inc.) criteria (Ungar and Gordon 1983) and were published as "VC" in Gordon (1991). The term "generic" means applicable to classes of equipment and activity rather than specific to particular items of equipment. These VC curves were then promulgated by the Institute of Environmental Sciences and Technology (IEST) for cleanroom design (IEST 1993) and were modified in 2005 (IEST 2005), as given in Table 2, mainly in terms of the one-third octave band RMS velocity spectra as defined in Equation 1), and they have been applied in a wide variety of technological fields until now. It is noted that VC-F and VC-G are to characterize very quiet spaces for some reasons and are not intended for use as design targets (Amick et al. 2005).

Another criterion, NIST-A, was firstly developed for the Advanced Measurement Laboratory at the U.S. National Institute of Standards and Technology (NIST) (Soueid, Amick, and Zsiraia 2005) and has become popular for nanotechnology to accommodate some of the ultra-high precision metrology, probe, and lithography equipment (Amick et al. 2005). It is identical to VC-E at frequencies above 20 Hz but maintains a constant RMS displacement amplitude at lower frequencies, as depicted in Table 2, making it very difficult to meet at sites subjected to significant low-frequency vibration.

Table 2. Definitions of generic VC curves and NIST-A criterion (after IEST 2005; Soueid, Amick, and Zsiraia 2005).

Criterion curve	*Detail size	Definition
VC-A	8 μm	260 μg between 4–8 Hz; 50 $\mu\text{m/s}$ between 8–80 Hz
VC-B	3 μm	130 μg between 4–8 Hz; 25 $\mu\text{m/s}$ between 8–80 Hz
VC-C	1–3 μm	12.5 $\mu\text{m/s}$ between 1–80 Hz
VC-D	0.1–0.3 μm	6.25 $\mu\text{m/s}$ between 1–80 Hz
VC-E	< 0.1 μm	3.1 $\mu\text{m/s}$ between 1–80 Hz
VC-F	N/A	1.6 $\mu\text{m/s}$ between 1–80 Hz
VC-G	N/A	0.78 $\mu\text{m/s}$ between 1–80 Hz
NIST-A	N/A	0.025 μm between 1–20 Hz; 3.1 $\mu\text{m/s}$ between 20–100 Hz

* The detail size refers to line width in the case of microelectronics fabrication, the particle (cell) size in the case of medical and pharmaceutical research, etc. It is not relevant to imaging associated with probe technologies, atomic force microscopes, and nanotechnology.

Modern light sources are designed to generate a beam with very low emittance and small beam size, which requires high mechanical stability of the girder assembly and low ground vibration level (Spataro, Lincoln, and Sharma 2018). To this end, a criterion in terms integrated RMS displacement as defined in Equation 3 was specified for the storage ring of National Synchrotron Light Source II (NSLS-II) at Brookhaven National Laboratory (BNL), US, giving D_{RMS} ($f = 4$ Hz) < 0.025 mm (25 nm) with $f_{max} = 50$ Hz (BNL 2007). The concerned frequency range is because the ground motion below 4 Hz is assumed to be correlated over the length of the storage ring cell, and that above 50 Hz is expected to be negligible (Spataro, Lincoln, and Sharma 2018).

3. Ground Vibrations Characteristics of Selected Teleseismic Earthquakes

3.1. Fourier Spectra and One-Third Octave RMS Velocity Spectra

A 1,000-second time history which that contained most of the notable shaking was extracted from each teleseism record, and then its Fourier spectrum and one-third octave RMS velocity spectrum were drawn to exhibit its frequency content. Additionally, the peak ground velocity (PGV) of each extracted velocigram and its predominant frequency (f_{pre}) obtained from the one-third octave spectrum instead of narrow-band Fourier spectrum for easier identification were listed in Table 3 for comparison.

Table 3. Characteristic parameters of ground vibrations induced by selected teleseismic earthquakes.

(a) 2011 Mw 9.1 JPEQ						
Station	HSNB			TAIB		
Dir.	EW	NS	V	EW	NS	V
f_{pre} (Hz)	0.050	0.050	0.040	0.063	0.080	0.050
PGV (cm/s)	0.884	1.284	0.564	1.274	0.828	0.642
(b) 2011 Mw 7.9 JPEQ						
Station	HSNB			TAIB		
Dir.	EW	NS	V	EW	NS	V
f_{pre} (Hz)	0.063	0.063	0.063	0.050	0.050	0.050
PGV (cm/s)	0.274	0.236	0.175	0.213	0.249	0.178
(c) 2011 Mw 6.9 MMEQ						
Station	HSNB			TAIB		
Dir.	EW	NS	V	EW	NS	V
f_{pre} (Hz)	0.160	0.125	0.080	0.100	0.080	0.080
PGV (cm/s)	0.434	0.376	0.147	0.235	0.326	0.123

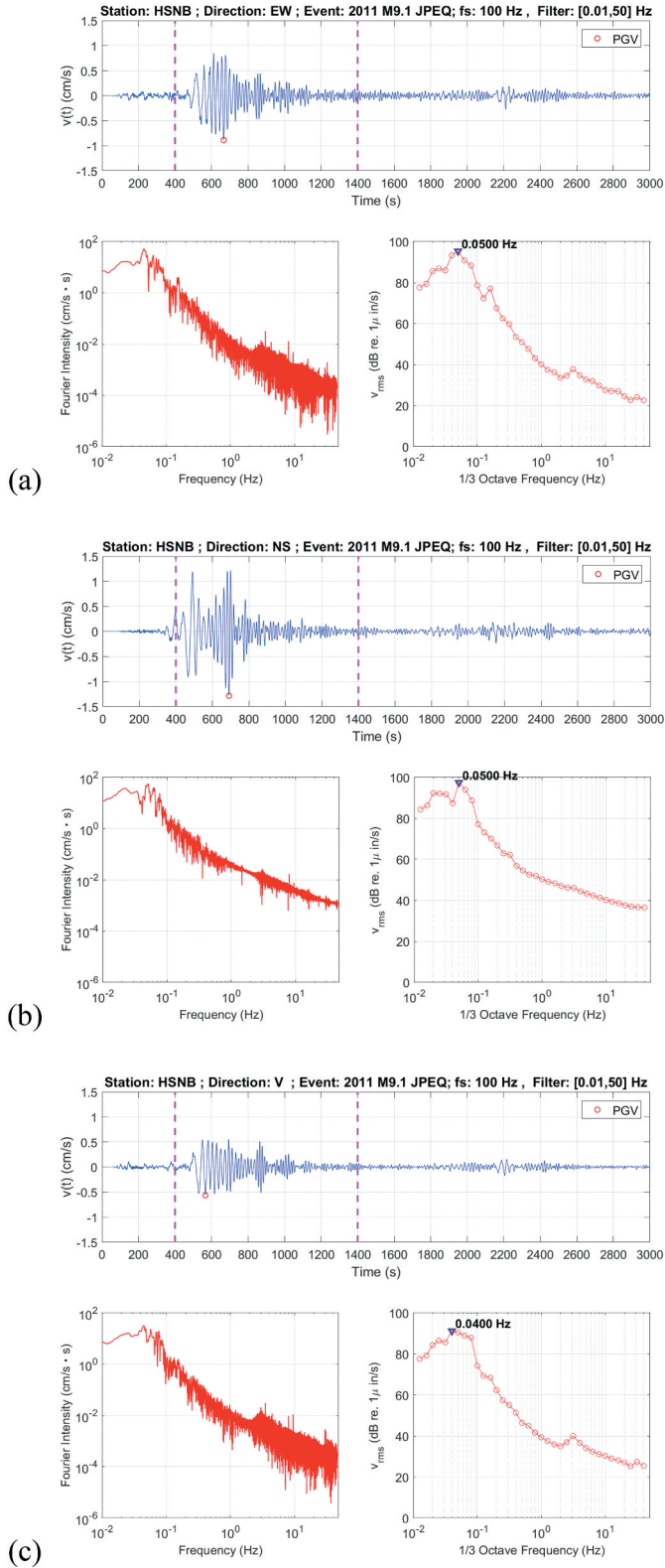


Figure 2. Velocity time histories, Fourier spectra, and one-third octave RMS velocity spectra of 2011 M_w 9.1 JPEQ at HSNB station: (a) EW-dir, (b) NS-dir, and (c) V-dir.

3.1.1. 2011 M_w 9.1 JPEQ

Figure 2 shows the velocity time histories, Fourier spectra, and one-third octave RMS velocity spectra (in dB) of the teleseisms in the east-west, the north-south, and the vertical directions (abbreviated as EW-dir, NS-dir, and V-dir hereafter) at HSNB. Significant low-frequency shaking that lasted for more than 10 minutes are noticed, longer than near-field records probably because of the arrival time lag among different frequency content of the teleseismic waves. The velocigrams show that PGVs in EW-dir and NS-dir were close to or even over 1 cm/s, whereas vertical PGV in V-dir was merely around 0.5 cm/s. According to the spectra, most of the vibration energy is concentrated below the frequency of 1 Hz with $f_{pre} = 0.04\text{--}0.05$ Hz in all directions, around which the vibration level can be over 90 dB. On the other hand, vibration level at 1–10 Hz is generally lower than 50 dB in all directions, probably due to the decay of high-frequency content of teleseisms after over-2,000-km propagation.

Figure 3 gives the velocigrams and spectra at TAIB. Similarly, it shows low-frequency vibration with horizontal PGVs up to 1 cm/s and a vibration level that can exceed 90 dB around 0.02–0.08 Hz. Besides, f_{pre} of the teleseism seemed rarely influenced by the site geology even though there was large discrepancy between V_{S30} of these two sites which makes their NEHRP site categories quite different (see section 2.2). Although V_{S30} can be well related to the site fundamental frequency, which is a common parameter to characterize the site effects in general earthquakes (Hassani and Atkinson 2016), they both represent only the overall near-surface state. This is because V_{S30} only involves the ground properties up to the depth of 30 m by definition, and the site fundamental frequency is likely to be dominated by the interface of strata with considerable difference in shear wave velocity (Singh et al. 2017, 2020). However, when the teleseismic wave is of concern, its wavelength is so long that its characteristics are dominated by the seismic source and large-scale velocity structures rather than the near-surface velocity profile.

In general, this extraordinarily huge teleseismic earthquake occurred in Japan caused remarkable low-frequency ground vibration in both northern and southern Taiwan.

3.1.2. 2011 M_w 7.9 JPEQ

Figures 4–5 depict the velocigrams, Fourier spectra and one-third octave RMS velocity spectra of the teleseisms were observed at HSNB and TAIB, respectively. The observed shaking, which had PGVs ranged from 0.18 cm/s to 0.25 cm/s with horizontal ones higher than vertical ones, was not as significant as the previous event, whereas most of the vibration energy similarly concentrated at frequencies lower than 1 Hz with $f_{pre} = 0.063$ Hz at HSNB and $f_{pre} = 0.050$ Hz at TAIB, and vibration levels around f_{pre} reached 80–85 dB. The much less magnitude of this event led to the milder vibrations in all directions, yet values of f_{pre} were not much different from those of 2011 M_w 9.1 JPEQ. This was possibly due to not only the similar faulting mechanism of the mainshock and aftershock, but also the comparable order of their focal depths (see Table 1) considering the more than 2,000 km epicentral distances of both events.

3.1.3. 2011 M_w 6.9 MMEQ

The velocigrams and spectra at HSNB and TAIB are shown in Figs. 6–7, respectively. More obvious waveforms as well as considerably larger horizontal PGVs than 2011 M_w 7.9 JPEQ are noticed despite the smaller magnitude of this event along with an epicentral distance at roughly same order, yet the vertical PGVs were smaller at both stations. Besides, the spectra depict somewhat higher f_{pre} around 0.08–0.16 Hz, and those at the HSNB site that has a larger V_{S30} are higher than at TAIB, showing that f_{pre} might be somewhat dependent on the site geology in this case with higher values of f_{pre} than previous ones. This is possibly because relatively shorter wavelengths were involved. Noted that the wavelengths were still much larger than 30 m, and therefore, the higher f_{pre} values at HSNB were probably not directly caused by larger V_{S30} , but should be attributed to a larger-scale velocity structure

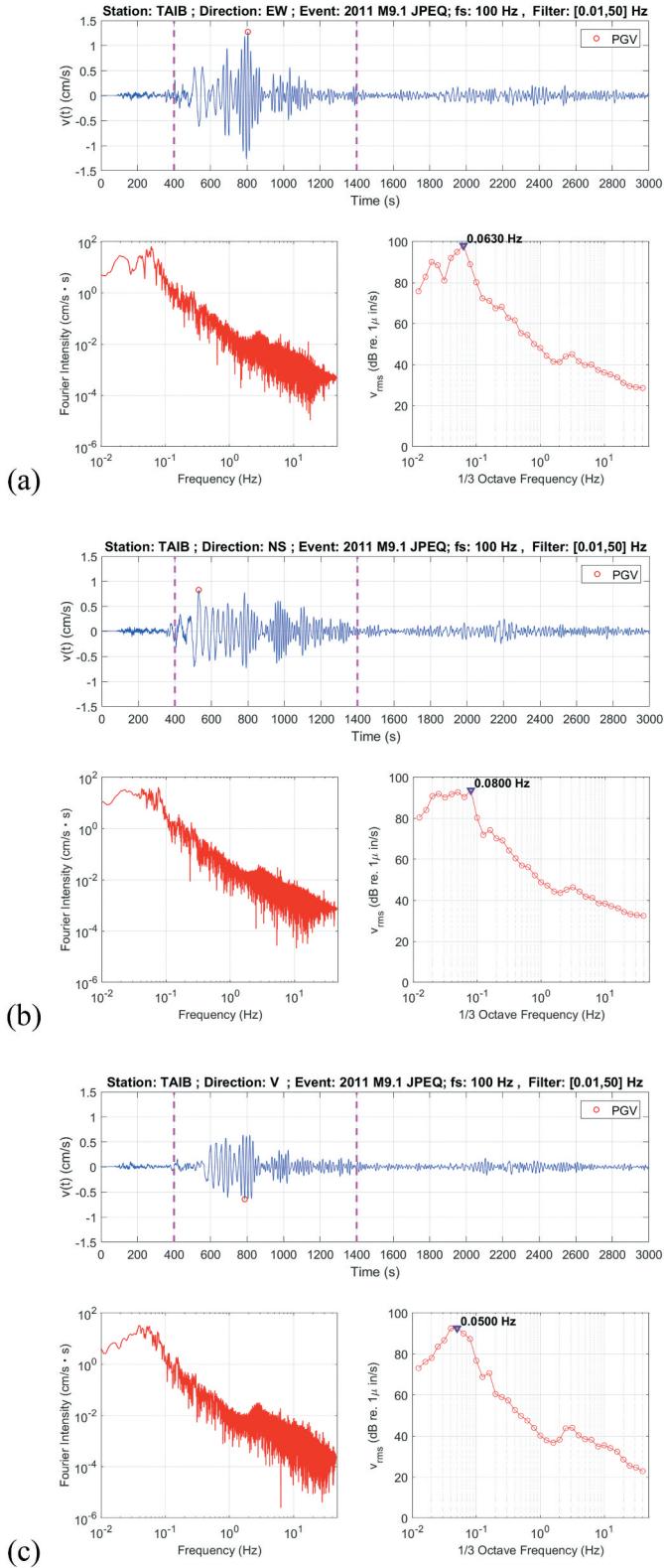


Figure 3. Velocity time histories, Fourier spectra, and one-third octave RMS velocity spectra of 2011 M_w 9.1 JPEQ at TAIB station: (a) EW-dir, (b) NS-dir, and (c) V-dir.

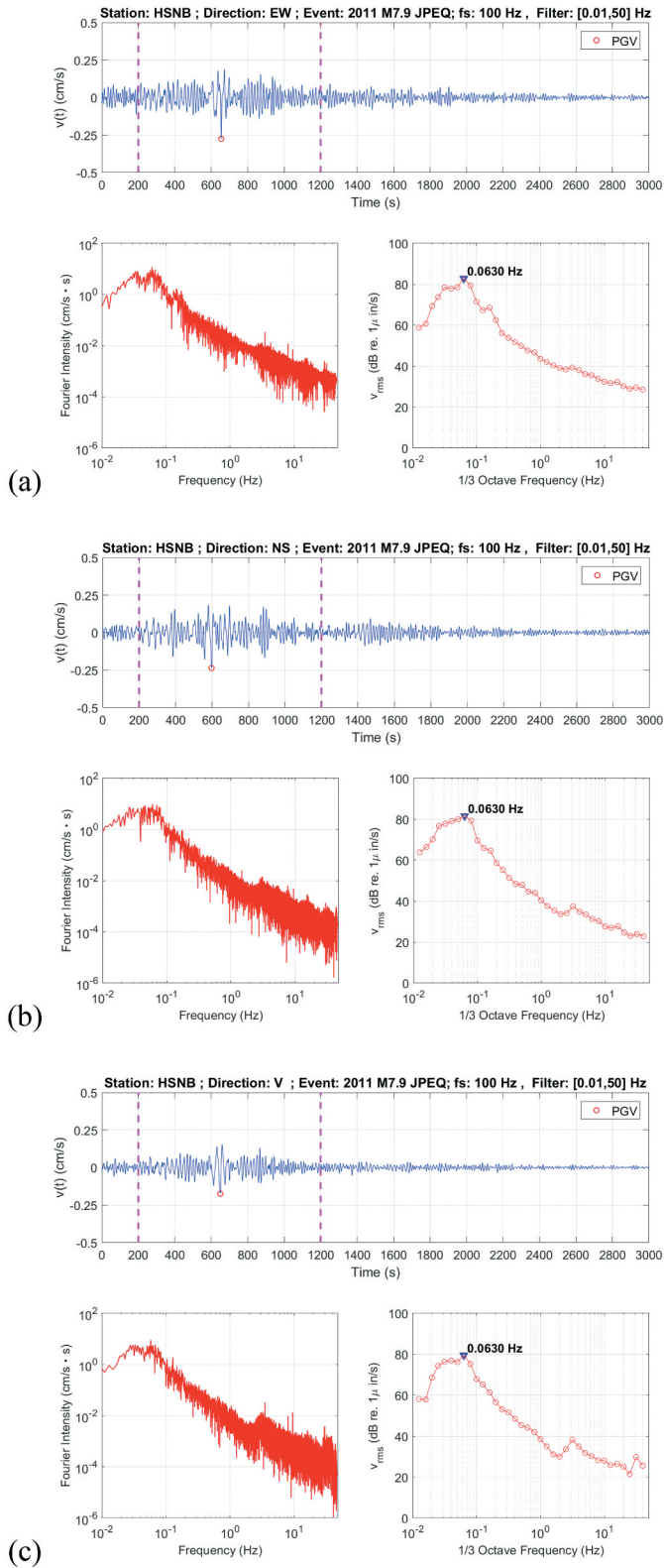


Figure 4. Velocity time histories, Fourier spectra, and one-third octave RMS velocity spectra of 2011 M_w 7.9 JPEQ at HSNB station: (a) EW-dir, (b) NS-dir, and(c) V-dir.

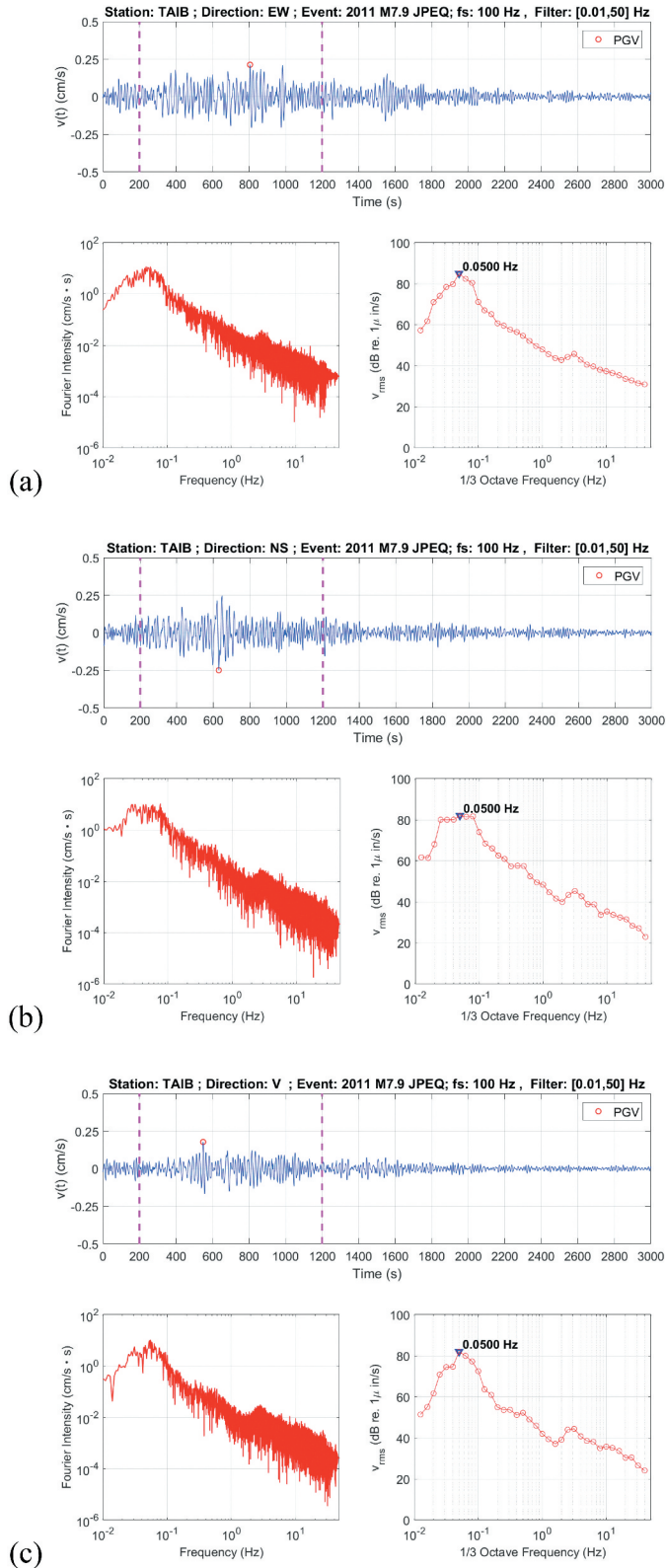


Figure 5. Velocity time histories, Fourier spectra, and one-third octave RMS velocity spectra of 2011 M_w 7.9 JPEQ at TAIB station: (a) EW-dir, (b) NS-dir, and (c) V-dir.

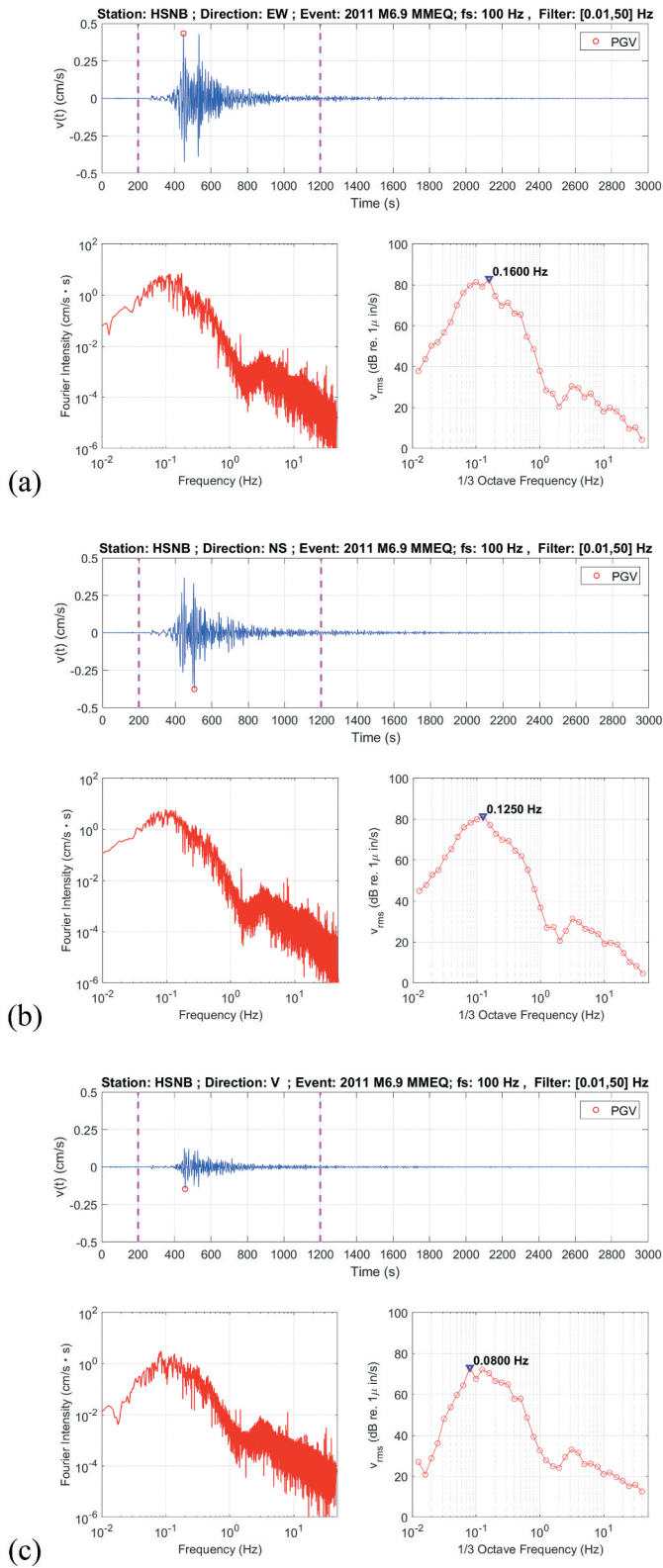


Figure 6. Velocity time histories, Fourier spectra, and one-third octave RMS velocity spectra of 2011 M_w 6.9 MMEQ at HSNB station: (a) EW-dir, (b) NS-dir, and (c) V-dir.

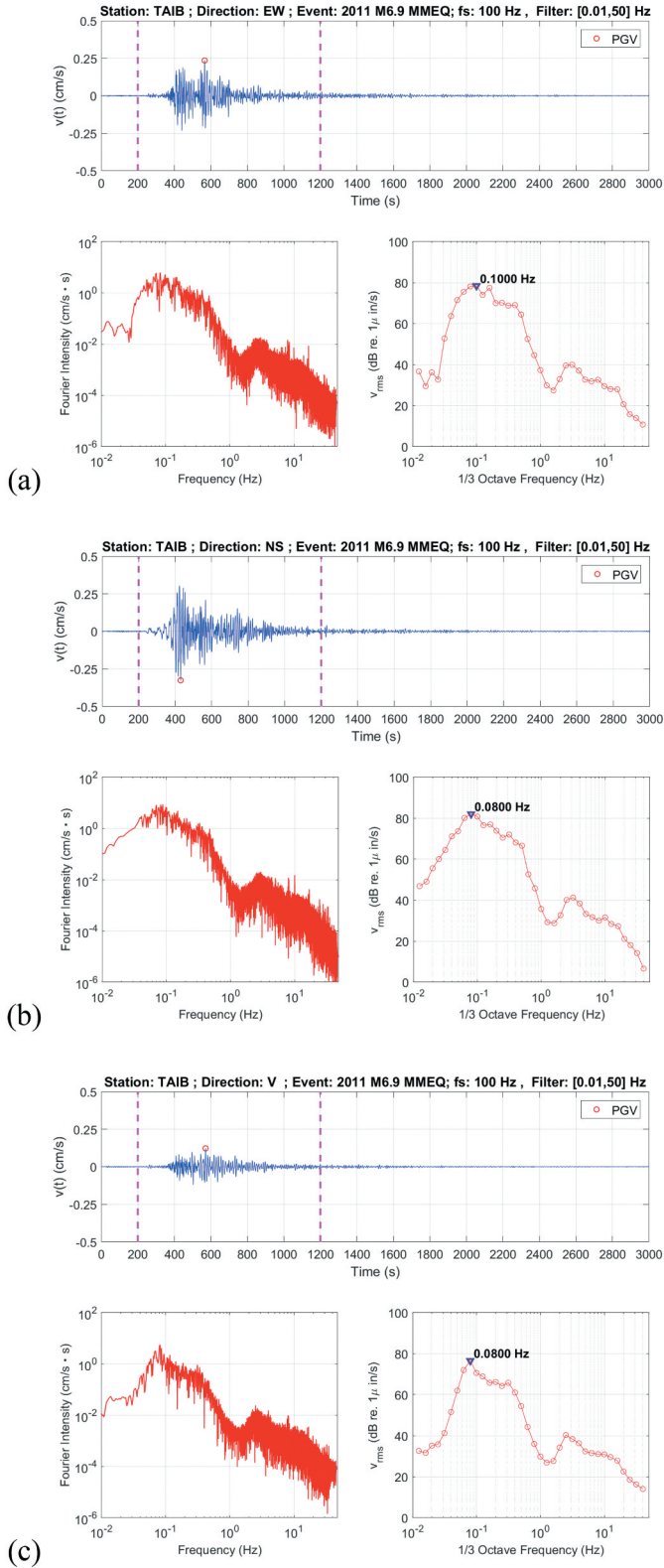


Figure 7. Velocity time histories, Fourier spectra, and one-third octave RMS velocity spectra of 2011 M_w 6.9 MMEQ at TAIB station: (a) EW-dir, (b) NS-dir, and (c) V-dir.

than what V_{S30} was associated. Nevertheless, the velocity structure at moderately deeper strata (up to several hundreds of meters) may have a strong positive correlation to V_{S30} (Boore, Thompson, and Cadet 2011).

The larger horizontal PGVs and higher f_{pre} of this event than 2011 M_w 7.9 JPEQ were presumed to be relevant to its relatively shallower source. The less than 10 km depth of the source made the propagation of seismic waves more concentrated near the surface with less reflections in the crust and less refraction to the deeper parts of the Earth, leading to less attenuation of the higher-frequency content of teleseismic waves during propagation. Furthermore, the epicenter was located at the west end of the strike-slip Nam Ma fault (with a strike of $N70^\circ E$) that caused this earthquake (Tun et al. 2014), which implied that the forward directivity of its source rupture was to the east-northeast (that is, toward Taiwan, as shown in Fig. 1), and this perhaps also contributed to the larger horizontal PGVs. Besides, the nearly pure left-lateral motion of the fault (Tun et al. 2014) might account for the smaller vertical PGVs compared with the reverse-faulting 2011 M_w 7.9 JPEQ.

3.2. Response Spectra

The 1,000-second time history from each teleseism record for spectral analysis was also used for response spectrum calculation. Figure 8a,b depicts the response spectra in terms of S_a , S_{va} , and S_d of the three investigated teleseismic earthquakes at HSNB and TAIB, respectively. Their features are interpreted as follows.

3.2.1. 2011 M_w 9.1 JPEQ

The maximum responses occurred at the periods of around 12.5–25 sec., which is generally conformable to f_{pre} listed in Table 3, indicating that the dominant frequency content of excitation considerably influences the response of structures. However, in some cases, significant displacement response appeared at a longer period around 40–50 sec., such as NS-dir and V-dir at HSNB as well as EW-dir and NS-dir at TAIB. They can be related to the minor peaks around 0.02–0.025 Hz in one-third octave RMS velocity spectra, implying that the low-frequency component of excitation has great contribution to the displacement response. Fortunately, this kind of vibration displacement is relevant to long-wavelength teleseismic waves and is thus less influential to facilities. Considering the JMA intensity scale for long-period ground motions (Sakai 2015), values of S_{va} within the period range of 1.5–8 sec in all directions at both stations are smaller than 5 cm/s, the threshold of the lowest intensity level. Therefore, in spite of a M_w of 9.1, this teleseismic earthquake was insufficient to cause any structural or non-structural damage or disorder.

3.2.2. 2011 M_w 7.9 JPEQ

Similarly, peak acceleration and velocity response generally occurred at periods corresponding to f_{pre} , whereas peak displacement might appear at longer periods where noticeable yet not dominant frequency content of the teleseisms existed. Furthermore, the smaller responses during this event than in its mainshock are far below the threshold of the lowest JMA intensity level for long-period ground motions.

3.2.3. 2011 M_w 6.9 MMEQ

Because of the higher f_{pre} of the teleseisms in this event, the maximum responses occurred at shorter periods (around or even below 10 sec) than in 2011 M_w 7.9 JPEQ, yet still remarkable displacement responses might appear at somewhat longer periods. Additionally, at TAIB, the maximum acceleration response occurred at a shorter period of 2–3 sec, implying that acceleration response could be more sensitive to relatively higher-frequency excitations. Regarding the JMA intensity scale for long-period ground motions, though in this event, the peaks of S_{va} may exhibit below 8 sec at HSNB, they are still lower than the threshold of the lowest level.

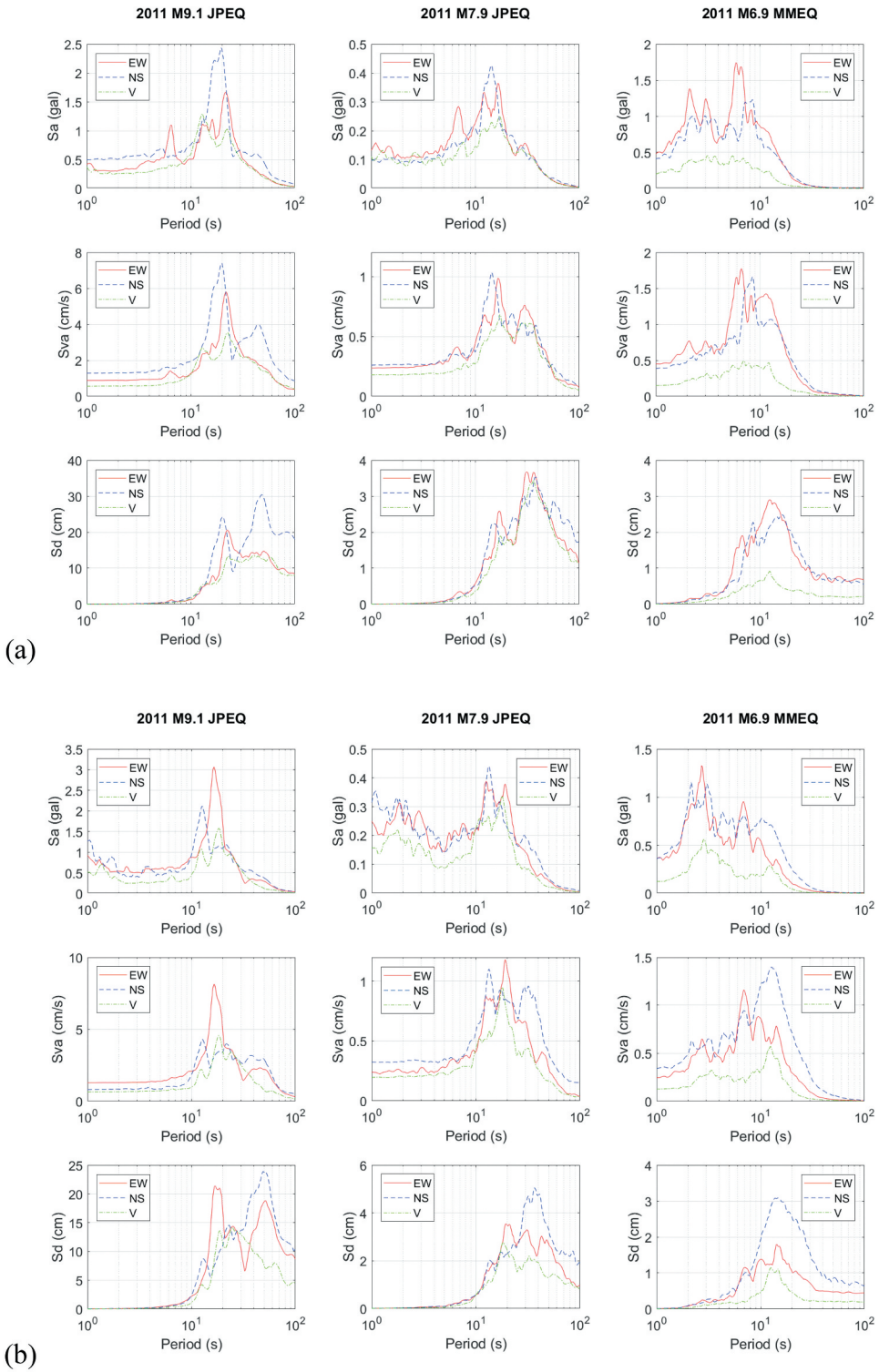


Figure 8. S_a , S_{va} , and S_d of the three investigated teleseismic earthquakes: (a) at HSNB station; and (b) at TAIB station.

4. Impact Assessment of Teleseisms on Vibration-Sensitive Facilities

To assess the possible impact of the investigated teleseismic earthquakes to vibration-sensitive facilities, such as those in the science parks near the adopted broadband seismic stations, the widely used generic VC curves (IEST 2005) and NIST-A criterion (Soueid and Amick 2005) were introduced. It is noted that only the VC-E curve of the former was used because looser ones could be insufficient for modern industrial need, while stricter ones are usually not for design demand. Then, the one-third octave RMS velocity of the observed ground vibrations were compared with these two criteria. In addition, the criterion in terms of displacement for NSLS-II was also included for comparison with the integrated RMS displacement.

4.1. 2011 M_w 9.1 JPEQ

Figure 9a,b shows the comparison between the observed vibration levels of the teleseisms and adopted vibration criteria at HSNB and TAIB, respectively. It is noted that the comparison of the one-third octave RMS velocity with VC-E and NIST-A criteria was made at the frequency range of 1–40 Hz based on the applicable range of these criteria, the pass band of the filter used in this study, and the definition of one-third octave bands as well, whereas for the integrated RMS displacement, the frequency range of comparison with the NSLS-II criterion was from 4 Hz to 50 Hz.

At HSNB, the VC-E criterion was exceeded only by the teleseism in NS-dir (with a larger PGV than in EW-dir) at frequencies of 1–7 Hz, whereas teleseisms at TAIB exceeded the VC-E criterion at most of the frequencies between 1 Hz and 5 Hz for horizontal ones and at 2.5–3.15 Hz for the vertical one. At the concerned frequency range of the adopted vibration criteria, the site geology seemed somewhat influential to the vibration level because a stiffer site suffered lower level of vibration.

On the other hand, the RMS velocity spectra were over the NIST-A criterion for frequencies lower than 15 Hz in NS-dir and lower than 7 Hz in both EW-dir and V-dir at HSNB, whereas at TAIB, the NIST-A criterion was exceeded for frequencies lower than 10 Hz in all directions. In addition, the NSLS-II criterion was also exceeded below the frequencies similar to those for NIST-A. As mentioned, the NIST-A criterion is identical to VC-E above 20 Hz yet holds a constant RMS displacement amplitude between 1–20 Hz, where it can be regarded as a criterion in terms of displacement. Therefore, this remarkably huge teleseismic event caused over-displacement at both stations in all directions considering both NIST-A and NSLS-II criteria.

4.2. 2011 M_w 7.9 JPEQ

Figure 10a,b depicts the comparison between the observed vibration level and adopted vibration criteria at HSNB and TAIB, respectively. The VC-E criterion was exceeded only by the teleseism in EW-dir at frequencies of 1–1.25 Hz at HSNB, whereas at TAIB, it was exceeded by teleseisms in all directions at part or all of the range between 1–4 Hz, also implying the influence of site geology. Despite the smaller magnitude of this event, all components of the teleseisms at both stations were beyond both displacement criteria at lower frequencies, including NIST-A at the range of 1–20 Hz and NSLS-II. It is also noted that the frequency range of exceedance was larger at TAIB (up to about 10 Hz), revealing again the site effect.

4.3. 2011 M_w 6.9 MMEQ

The comparison of the observed vibration level with adopted vibration criteria at HSNB and TAIB are given in Fig. 11a,b, respectively. There was no teleseism in any direction beyond the VC-E criterion at both stations in this event, but those at TAIB were closer to the threshold. On the other hand, the NIST-A criterion was generally exceeded at HSNB for frequencies of 1–4 Hz, whereas the NSLS-II

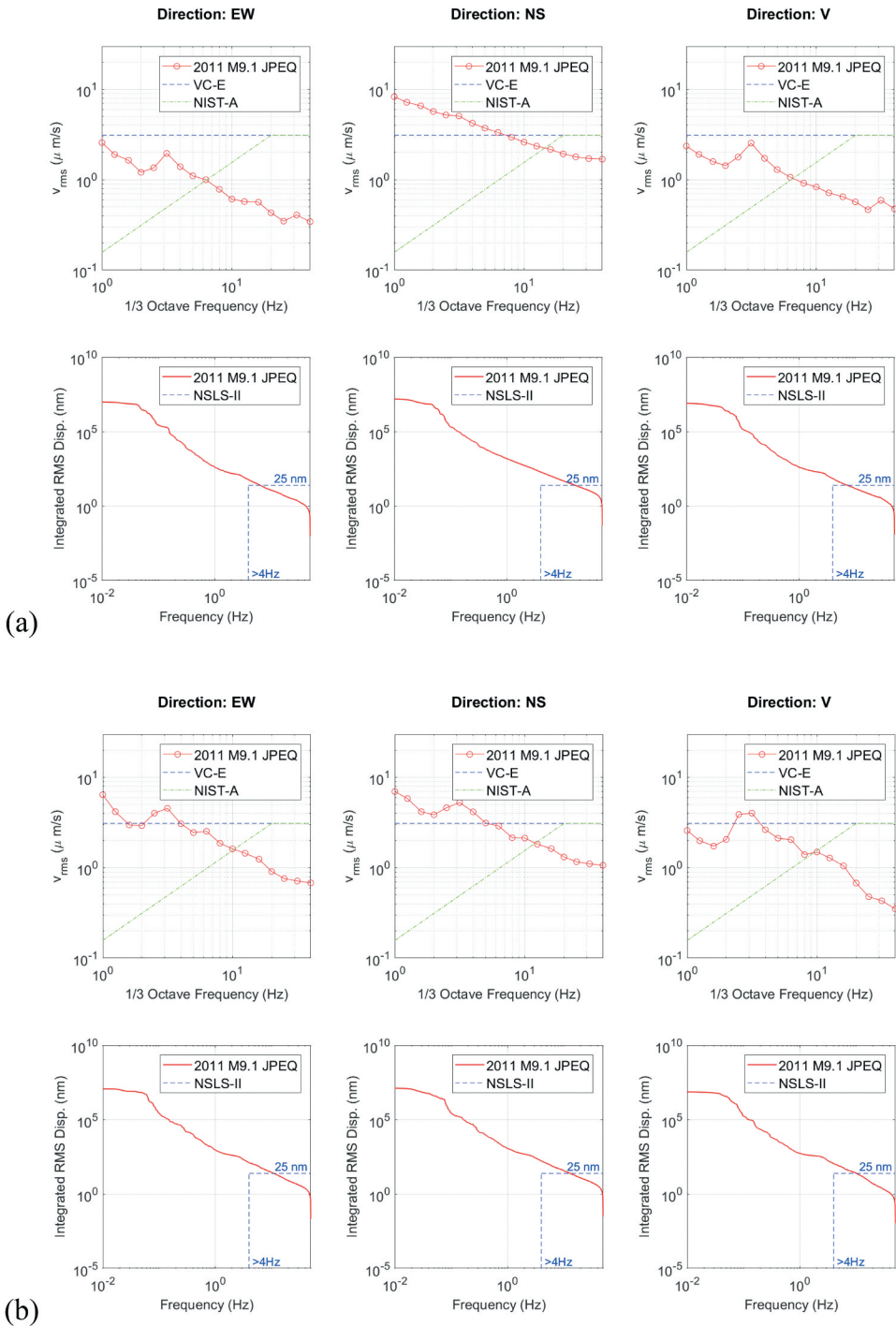


Figure 9. Comparison of one-third octave RMS velocity spectra and integrated RMS displacement of 2011 M_w 9.1 JPEQ with vibration criteria: (a) at HSNB station; and (b) at TAIB station.

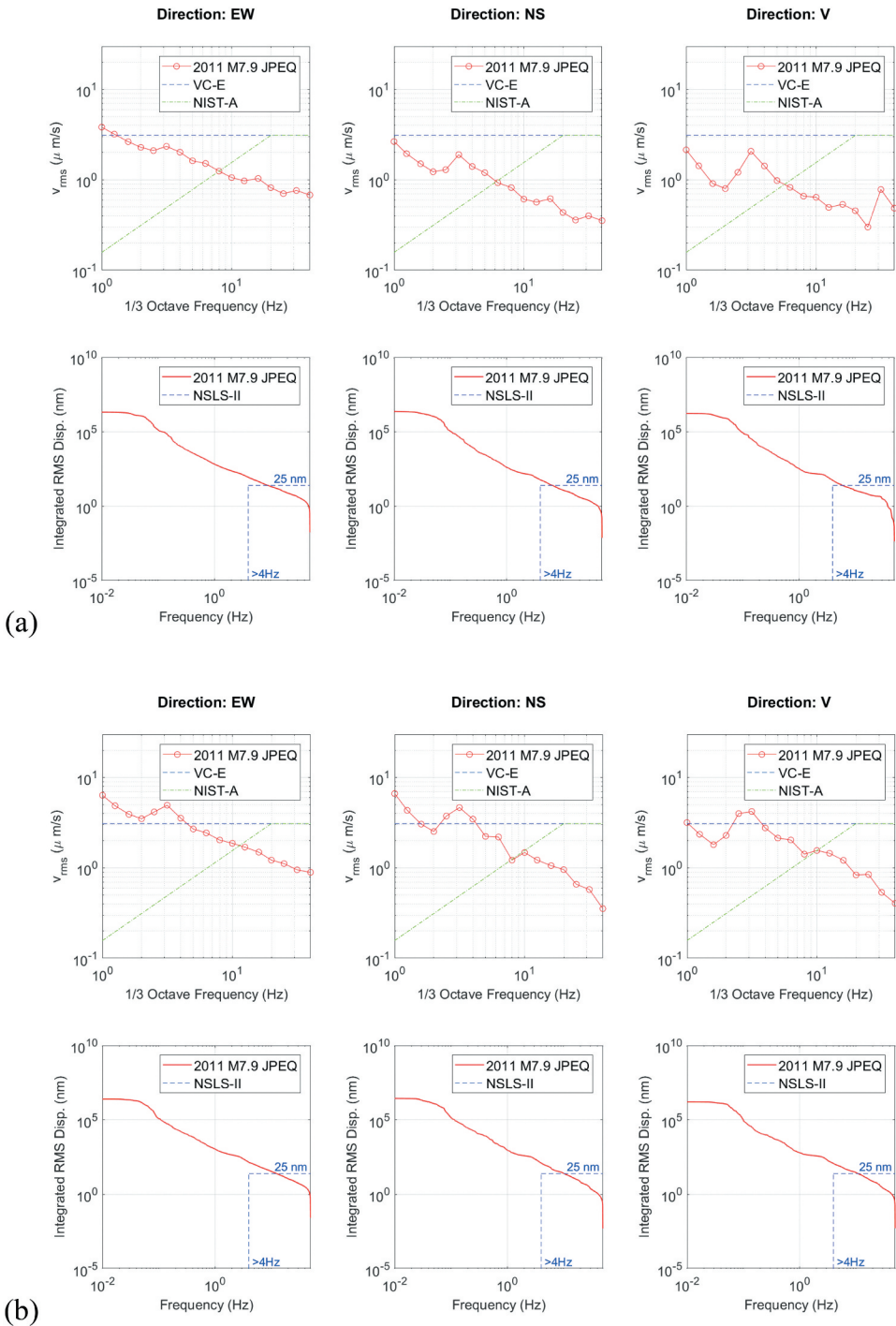


Figure 10. Comparison of one-third octave RMS velocity spectra and integrated RMS displacement of 2011 M_w 7.9 JPEQ with vibration criteria: (a) at HSNB station; and (b) at TAIB station.

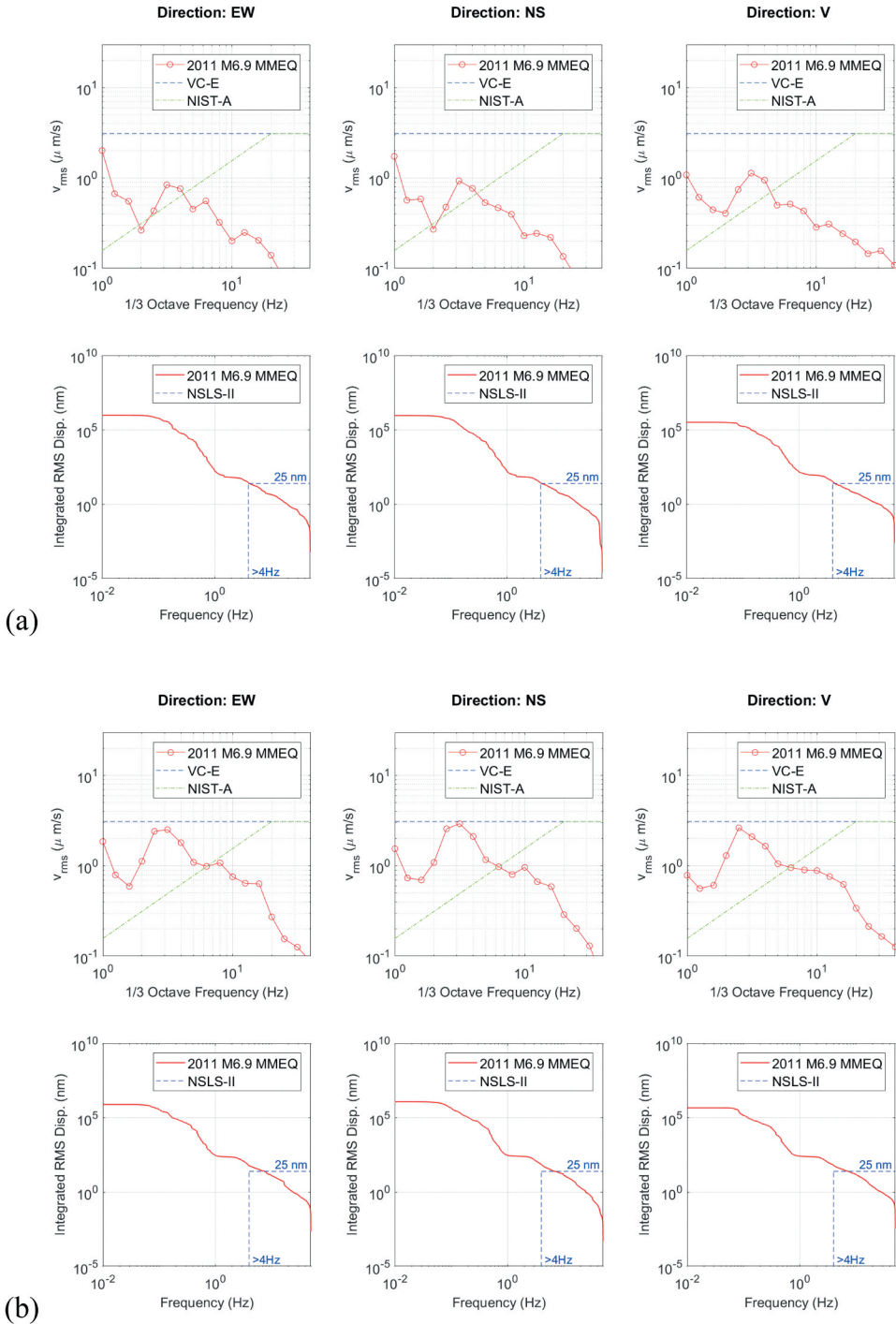


Figure 11. Comparison of one-third octave RMS velocity spectra and integrated RMS displacement of 2011 M_w 6.9 MMEQ with vibration criteria: (a) at HSNB station; and (b) at TAIB station.

criterion was only reached or exceeded at nearly 4 Hz. Nevertheless, all the components of teleseisms at TAIB were above both displacement criteria at a wider frequency range to a more notable extent than HSNB probably due to the site effect.

4.4. Discussions

In general, the VC-E criterion can only be exceeded by teleseismic earthquakes having large enough magnitudes; among the investigated events with an epicentral distance of over 2,000 km, the M_w 6.9 one was insufficient to induce over-criterion ground vibration. On the other hand, the displacement criteria, including the NIST-A criterion within the frequency range of 1–20 Hz and that for NSLS II, were exceeded in all the examined teleseisms. Although this is not surprising because displacement criteria are difficult to meet when low-frequency vibrations such as teleseisms are concerned, the possible impact of teleseisms on facilities very sensitive to vibrations is thus revealed. Fortunately, the travelling time of teleseismic shear waves, which was approximately 8–9 minutes for the three examined teleseismic events (CWB 2021), enables the operators of these facilities to be prepared as long as proper emergency procedure has been established.

The below-1-Hz frequency content of the ground vibration is usually considered less influential for its corresponding to longer wavelength and is not covered in the adopted vibration criteria. However, the integrated RMS displacement curves showed that the abundant content of the investigated teleseisms at frequencies < 1 Hz had significant contribution to vibration displacement. Besides, according to Section 3.1, the vibration levels of these teleseisms were much larger at the frequencies < 1 Hz than those ≥ 1 Hz. Therefore, caution may be required on the below-1-Hz content of teleseisms for facilities that are sensitive to vibrational displacement and have very large dimensions (e.g. huge particle accelerators) rested on soft sites in establishing their design requirements and vibration mitigation strategies.

Unlike f_{pre} of the teleseisms, which was only somewhat dependent on the site geology in 2011 M_w 6.9 MMEQ, the vibration level concerning the adopted vibration criteria was higher in all cases at the softer site (with a lower V_{S30}) TAIB. This is probably because these vibration criteria are defined within the frequency range of 1–100 Hz, which can be considered overlapped with the general range of fundamental frequency of the ground. Consequently, near-surface geology of the site could be decisive regarding the vibration impact assessment.

5. Conclusions

This paper presented the investigation of the ground vibration during three teleseismic earthquakes in 2011 observed at two broadband seismic stations near major science parks in Taiwan. Based on the characteristics of teleseisms revealed by Fourier spectra, one-third octave band spectra, and response spectra, as well as their comparison with three widely used vibration criteria, the following conclusions can be drawn:

- (1) The teleseisms from 2011 M_w 9.1 Great East Japan earthquake and its M_w 7.9 aftershock, both relevant to a reverse faulting mechanism, had predominant frequencies that ranged from 0.04 to 0.08 Hz, which exhibited hardly noticeable difference between the two sites with quite different V_{S30} values probably because of the very long wavelengths. On the other hand, those of the 2011 M_w 6.9 Tarlay, Myanmar earthquake caused by strike-slip faulting with a shallower focal depth were between 0.08 and 0.16 Hz, higher than the previous two events possibly due to the discrepancies in focal properties, and higher at the site with a lower V_{S30} , showing that the predominant frequency of teleseisms might be somewhat dependent on the site geology in this case with relatively shorter wavelengths.
- (2) The significant peaks of response spectra occurred at low frequencies, which correlated well to the predominant frequencies of the teleseisms, showing their influence on structures with very long natural periods, whereas the acceleration response could be sensitive to relatively higher-

frequency content and remarkable displacement response could be induced by relatively lower-frequency content. However, compared with the JMA intensity scale for long-period ground motions, the structural response was insufficient to cause any damage or disorder.

- (3) Except for the 2011 Tarlay, Myanmar earthquake which had the smallest magnitude among the investigated events, the vibration levels were above the VC-E criterion in terms of one-third octave band RMS velocity in some of the components at certain frequencies. On the other hand, the displacement criteria including NIST-A criterion between 1–20 Hz and that of NSLS-II were exceeded in all cases, exhibiting the influence of low-frequency teleseisms on facilities very sensitive to vibrational displacement. In addition, vibration levels within the concerned frequency range of these vibration criteria (1–100 Hz) observed at the site with a lower V_{S30} were generally larger, showing the importance of near-surface site geology in assessing the impact of vibration.

Acknowledgments

The authors gratefully acknowledge the Central Weather Bureau (CWB), Taiwan, for providing valuable data of its broadband array and relevant information via the Geophysical Database Management System (GDMS). The authors also acknowledge the National Center for Research on Earthquake Engineering (NCREE) and CWB for their establishing the Engineering Geological Database for Taiwan Strong-Motion Instrument Program (EGDT, website: egdt.ncree.org.tw).

Disclosure Statement

No potential conflict of interest was reported by the author(s).

References

- Amick, H., M. Gendreau, T. Busch, and C. G. Gordon. 2005. Evolving criteria for research facilities: I – Vibration. Proceedings of SPIE 5933, Buildings for Nanoscale Research and Beyond San Diego, CA.
- Ammon, C. J., T. Lay, H. Kanamori, and M. Cleveland. 2011. A rupture model of the 2011 off the Pacific coast of Tohoku Earthquake. *Earth, Planets and Space* 63: 693–96. doi: [10.5047/eps.2011.05.015](https://doi.org/10.5047/eps.2011.05.015).
- Barberio, M. D., F. Gori, M. Barbieri, A. Billi, A. Caracausi, G. De Luca, S. Franchini, M. Petitta, and C. Doglioni. 2020. New observations in Central Italy of groundwater responses to the worldwide seismicity. *Scientific Reports* 10: 17850. doi: [10.1038/s41598-020-74991-0](https://doi.org/10.1038/s41598-020-74991-0).
- BNL (Brookhaven National Laboratory). 2007. *NSLS-II preliminary design report*. Upton, NY: Brookhaven National Laboratory.
- Boore, D. M., E. M. Thompson, and H. Cadet. 2011. Regional correlations of V_{S30} and velocities averaged over depths less than and greater than 30 m. *Bulletin of the Seismological Society of America* 101: 3046–59. doi: [10.1785/B0120110071](https://doi.org/10.1785/B0120110071).
- Bormann, P., M. Baumbach, M. Bock, H. Grosser, G. L. Choy, and J. J. Boatwright. 2013. Seismic sources and source parameters. In *New manual of seismological observatory practice (NMSOP-2)*, ed. P. Bormann, Chapter 3. Potsdam: Deutsches GeoForschungszentrum GFZ. doi:[10.2312/GFZ.NMSOP-2_ch3](https://doi.org/10.2312/GFZ.NMSOP-2_ch3).
- BSSC (Building Seismic Safety Council). 2003. *NEHRP recommended provisions for seismic regulations for new buildings and other structures*. 2003 ed. Part 1: Provisions (FEMA 450). Washington, DC: National Institute of Building Sciences.
- CWB (Central Weather Bureau). 2021. Geophysical database management system. Accessed September 6, 2021. <http://gdms.cwb.gov.tw/>.
- Dengler, L., and M. Sugimoto. 2011. *Learning from earthquakes—The Japan Tohoku Tsunami of March 11, 2011, EERI special earthquake report*. Oakland: Earthquake Engineering Research Institute.
- Estève, C., P. Audet, A. J. Schaeffer, D. Schutt, R. C. Aster, and J. Cubley. 2020. The upper mantle structure of northwestern Canada from teleseismic body wave tomography. *Journal of Geophysical Research: Solid Earth* 125 (2): e2019JB018837. doi: [10.1029/2019JB018837](https://doi.org/10.1029/2019JB018837).
- Furumura, T., and B. L. N. Kennett. 2019. The significance of long-period ground motion at regional to teleseismic distances from the 610-km deep M_w 8.3 Sea of Okhotsk earthquake of 24 May 2013. *Journal of Geophysical Research: Solid Earth* 124 (8): 9075–94. doi: [10.1029/2019JB018147](https://doi.org/10.1029/2019JB018147).
- Furumura, T., S. Takemura, S. Noguchi, T. Takemoto, T. Maeda, K. Iwai, and S. Padhy. 2011. Strong ground motions from the 2011 off-the Pacific-Coast-of-Tohoku, Japan ($M_w = 9.0$) earthquake obtained from a dense nationwide seismic network. *Landslides* 8: 333–38. doi: [10.1007/s10346-011-0279-3](https://doi.org/10.1007/s10346-011-0279-3).

- Gordon, C. G. 1991. Generic criteria for vibration-sensitive equipment. Proceedings of SPIE 1619, Vibration Control in Microelectronics, Optics, and Metrology San Jose, CA. doi: [10.1117/12.56826](https://doi.org/10.1117/12.56826).
- GÜRALP Systems. 2021. CMG-40TD broadband seismometer and digitiser. Accessed April 3, 2021. <https://www.guralp.com/documents/DAS-040-0003.pdf>.
- Gutenberg, B. 1945a. Amplitudes of surface waves and magnitudes of shallow earthquakes. *Bulletin of the Seismological Society of America* 35 (1): 3–12. doi: [10.1785/BSSA0350010003](https://doi.org/10.1785/BSSA0350010003).
- Gutenberg, B. 1945b. Amplitudes of P, PP, and S and magnitude of shallow earthquakes. *Bulletin of the Seismological Society of America* 35 (2): 57–69. doi: [10.1785/BSSA0350020057](https://doi.org/10.1785/BSSA0350020057).
- Gutenberg, B. 1945c. Magnitude determination of deep-focus earthquakes. *Bulletin of the Seismological Society of America* 35 (3): 117–30. doi: [10.1785/BSSA0350030117](https://doi.org/10.1785/BSSA0350030117).
- Hanson, C. E., D. A. Towers, and L. D. Meister. 2006. Transit Noise and vibration impact assessment. Report No. FTA-VA-90-1003-06, Federal Transit Administration, Washington, DC.
- Hassani, B., and G. M. Atkinson. 2016. Applicability of the site fundamental frequency as a V_{S30} proxy for Central and Eastern North America. *Bulletin of the Seismological Society of America* 106 (2): 653–64. doi: [10.1785/0120150259](https://doi.org/10.1785/0120150259).
- Hirose, F., K. Miyaoka, N. Hayashimoto, T. Yamazaki, and M. Nakamura. 2011. Outline of the 2011 off the Pacific coast of Tohoku Earthquake (M_w , 9.0)—Seismicity: Foreshocks, mainshock, aftershocks, and induced activity. *Earth, Planets and Space* 63: 513–18. doi: [10.5047/eps.2011.05.019](https://doi.org/10.5047/eps.2011.05.019).
- IENT (Institute of Environmental Sciences and Technology). 1993. *Considerations in cleanroom design, IES-RP-CC012.1*. Schaumburg: IEST.
- IENT (Institute of Environmental Sciences and Technology). 2005. *Considerations in clean room design, IES-RP-CC012.2*. Schaumburg: IEST.
- Kuo, C.-H., K.-L. Wen, -H.-H. Hsieh, C.-M. Lin, T.-M. Chang, and K.-W. Kuo. 2012. Site classification and V_{S30} estimation of free-field TSMIP stations using the logging data of EGD. *Engineering Geology* 129–130: 68–75. doi: [10.1016/j.enggeo.2012.01.013](https://doi.org/10.1016/j.enggeo.2012.01.013).
- Liu, C., M.-W. Huang, and Y.-B. Tsai. 2006. Water level fluctuations induced by ground motions of local and teleseismic earthquakes at two wells in Hualien, Eastern Taiwan. *Terrestrial, Atmospheric and Oceanic Sciences* 17 (2): 371–89. doi: [10.3319/TAO.2006.17.2.371\(T\)](https://doi.org/10.3319/TAO.2006.17.2.371(T)).
- Rawlinson, N., S. Pilia, M. Young, M. Salmond, and Y. Yang. 2016. Crust and upper mantle structure beneath southeast Australia from ambient noise and teleseismic tomography. *Tectonophysics* 689: 143–56. doi: [10.1016/j.tecto.2015.11.034](https://doi.org/10.1016/j.tecto.2015.11.034).
- Sakai, A. 2015. An expression of the seismic intensity level for long-period ground motion. *Journal of JSCE* 3: 160–73. doi: [10.2208/journalofjsce.3.1_160](https://doi.org/10.2208/journalofjsce.3.1_160).
- Shin, T.-C., C.-H. Chang, H.-C. Pu, H.-W. Lin, and P.-L. Leu. 2013. The geophysical database management system in Taiwan. *Terrestrial, Atmospheric and Oceanic Sciences* 24 (1): 11–18. doi: [10.3319/TAO.2012.09.20.01\(T\)](https://doi.org/10.3319/TAO.2012.09.20.01(T)).
- Singh, A. P., A. Shukla, M. R. Kumar, and M. G. Thakkar. 2017. Characterizing surface geology, liquefaction potential, and maximum intensity in the Kachchh Seismic Zone, Western India, through microtremor analysis. *Bulletin of the Seismological Society of America* 107 (3): 1277–92. doi: [10.1785/0120160264](https://doi.org/10.1785/0120160264).
- Singh, A. P., B. Sairam, V. Pancholi, S. Chopra, and M. R. Kumar. 2020. Deccan Volcanic Province of western India through microtremor analysis. *Soil Dynamics and Earthquake Engineering* 138: 106348. doi: [10.1016/j.soildyn.2020.106348](https://doi.org/10.1016/j.soildyn.2020.106348).
- Soueid, A., H. Amick, and Zsiraia, T. 2005. Addressing the environmental challenges of the NIST advanced measurement laboratory. Proceedings of SPIE 5933, Buildings for Nanoscale Research and Beyond San Diego, CA.
- Spataro, C. J., F. C. Lincoln, and S. K. Sharma. 2018. NSLS-II site vibration studies to characterize beamline stability. Paper presented at the 10th International Conference of Mechanical Engineering Design of Synchrotron Radiation Equipment and Instrumentation (MEDSI2018), Paris, France. doi: [10.18429/JACoW-MEDSI2018-WEPH29](https://doi.org/10.18429/JACoW-MEDSI2018-WEPH29).
- Tun, S. T., Y. Wang, S. N. Khaing, M. Thant, N. Htay, Y. M. M. Htwe, T. Myint, and K. Sieh. 2014. Surface ruptures of the M_w 6.8 March 2011 Tarlay Earthquake, Eastern Myanmar. *Bulletin of the Seismological Society of America* 104 (6): 2915–32. doi: [10.1785/0120130321](https://doi.org/10.1785/0120130321).
- Ungar, E. E., and C. G. Gordon. 1983. Vibration challenges in microelectronics manufacturing. *Shock and Vibration Bulletin* 53 (1): 51–58.
- USGS (United States Geological Survey). 2021. Earthquake hazards program. Accessed September 6, 2021. <http://earthquake.usgs.gov/>.
- Yasuda, S., K. Harada, K. Ishikawa, and Y. Kanemaru. 2012. Characteristics of liquefaction in Tokyo Bay area by the 2011 Great East Japan Earthquake. *Soils and Foundations* 52 (5): 793–810. doi: [10.1016/j.sandf.2012.11.004](https://doi.org/10.1016/j.sandf.2012.11.004).